Quantitative proteome and PTMome analysis of *Arabidopsis thaliana* root responses to persistent osmotic and salinity stress.

Rodriguez, MC.[1*]., Mehta, D[1*]., Tan, M[1], and Uhrig, RG[1]

[#]Corresponding Authors:

*Denotes equal contribution

Dr. R. Glen Uhrig

Department of Biological Sciences
University of Alberta
Edmonton, Alberta
Canada
T6G 2E9

Phone: +1 780 492 3088
E-Mail: ruhrig@ualberta.ca

[1]Department of Biological Sciences, University of Alberta, Edmonton, Alberta, Canada

Running Title: Impact of Salt and Osmotic Stress on Root Proteome

ABSTRACT

Environmental conditions contributing to abiotic stress such as drought result in large annual economic losses around the world. As sessile organisms, plants cannot escape the environmental stresses they encounter, but instead must adapt to survive. Studies investigating plant responses to osmotic and/or salt stress have largely focused on short-term systemic responses, leaving our understanding of intermediate to longer-term adaptation (24 h - days), less well understood. In addition to protein abundance and phosphorylation changes, evidence suggests reversible protein acetylation may also be important for abiotic stress responses. Therefore, to characterize protein-level effects of osmotic and salt stress, we undertook a label-free proteomic analysis of *Arabidopsis thaliana* roots exposed to 300 mM Mannitol and 150 mM NaCl for 24 hours. We assessed protein phosphorylation, acetylation and changes in abundance, detecting significant changes in the status of 106, 66 and 447 proteins, respectively. Comparison with available transcriptome data from analogous treatments, indicate that transcriptome- and proteome-level changes occur in parallel. Furthermore, significant changes in abundance, phosphorylation and acetylation involve different proteins from the same networks, indicating a concerted, multifaceted regulatory approach to prolonged osmotic and/or salt stress. Lastly, our quantitative proteomic approach uncovered a new root elongation protein, Armadillo repeat protein 2 (ARO2), which exhibits a salt stress dependent phenotype. Collectively, our findings indicate dynamic protein-level changes continue to occur in plant roots 24 hours from the onset of osmotic and salt stress and that these changes differ across multiple levels of the proteome.

Key Words: ***Arabidopsis thaliana,*** **Protein Acetylation, Protein Phosphorylation, Post-Translational Modifications, Quantitative Proteomics**

INTRODUCTION

Environmental conditions contributing to abiotic stresses such as drought and salinity result in large annual economic losses around the world. Between 2005 and 2015, drought was responsible for 30 % of agricultural loss, totaling to USD 19.5 billion (Food and Agriculture Organization of the United Nations (FAO), 2017). The combined result of human activities and climate change represent two of the major environmental factors currently threatening global food security (Ghosh and Xu, 2014), with rising global temperatures extending drought periods and lengthening plant drought recovery time (Schwalm et al., 2017). More frequent and severe droughts have left farmers to depend on progressively unsustainable irrigation and fertilization practices to maintain crop yield, placing further stress on drainage patterns and salinity levels of farmland (Kaushal et al., 2018). Both drought and salinity stress create a hyperosmotic condition typically referred to as osmotic stress, while increased salinity has the additive effect of concurrently increasing ionic strength. These osmotic and ionic effects massively impede the ability of roots to take up water, forcing molecular, cellular and/or morphological changes in order to adapt and survive.

All plant organs must adapt to drought and salt stress; however, roots are at the frontlines and are thus responsible for adjusting their molecular program as necessary to ensure whole plant survival. In particular, under water-limiting conditions, roots restructure their investment from lateral root formation to axile roots to forage deeper soil layers (Paez-Garcia et al., 2015). For example, overexpression of the cell wall expansion protein EXPA5, stimulates root cell elongation by lengthening the root tip rather than increasing cell number (Xu et al., 2014). While DEEPER ROOTING 1 (DRO1), a rice quantitative trait locus, is capable of increasing root angle in response to gravity, creating a steeper and deeper root system architecture, in addition to a higher photosynthetic capability, less wilting, and a >30 % increase in filled grain under severe drought (Uga et al., 2013). Thus, root system changes help define the growth and structure of aboveground biomass.

Within all plant cells, proteins are at the heart of sensing and initiating signaling events that then launch stress-adaptive responses. While the majority of our understanding of drought responses has been driven by transcriptomic responses (Kreps et al., 2002; Killan et al 2007), understanding a plant's environmental stress response and adaptation over time at the protein-level through quantitative proteomics, offers new opportunities for both fundamental understanding and biotechnological application.

Osmotic and salt stress have a major influence over crop productivity worldwide (Ashraf and Akram, 2009), making it essential that we continue to refine our understanding of how plants respond to these perturbations in order to breed and/or engineer more climate resilient crops. Emphasizing this need are the multiple studies that have examined the effects of osmotic and/or salt stress across a range of photosynthetic eukaryotes using both global and targeted analyses to understand the range of molecular, biochemical, physiological and morphological responses these stresses elicit (Zhang et al., 2012). This compendium of osmotic and salt stress data encompass a vast multitude of plant systems, time-frames and applied technologies, ranging from minutes to days of stress exposure (Jiang et al., 2007), followed by transcriptomic (Kilian et al., 2007; Kreps et al., 2002; Rest et al., 2016; Yin et al., 2019), proteomic (Jiang et al., 2007; Koh et al., 2015; Luo et al., 2015; Zhang et al., 2012) and metabolomic (Shelden et al., 2016) analyses to assess how the root environment responds to either abiotic stress. However, given the large variability in sampling time frames and root growth approaches, coupled with the: 1) limited in-parallel examination of multiple stresses and proteoforms within the

same study, 2) known disconnect between changing transcripts and proteins (Baerenfaller et al., 2012; Petricka et al., 2012; Reiland et al., 2009; Seaton et al., 2018; Uhrig et al., 2019) and 3) limited investigations of the role post-translational modifications (PTMs) play in root osmotic and salt adaptation (Koh et al., 2015; Wu et al., 2016; Zhu, 2016), further quantitative proteomic analysis are required.

PTMs are a pillar of properly functioning eukaryotic cells. Of the known PTMs, protein phosphorylation and acetylation are the two most abundant (Choudhary et al., 2009; Henriksen et al., 2012; Sharma et al., 2014; Uhrig et al., 2019; Weinert et al., 2011), with plants maintaining a comparable phosphoprotein landscape to humans (PhosPhat, http://phosphat.uni-hohenheim.de/; (Heazlewood et al., 2008), ATHENA; http://athena.proteomics.wzw.tum.de/; (Mergner et al., 2020); Plant PTM Viewer, https://www.psb.ugent.be/webtools/ptm-viewer/; (Willems et al., 2019). More recently, global analysis of protein acetylation in Arabidopsis (Finkemeier et al., 2011; Hartl et al., 2017; Liu et al., 2018; Uhrig et al., 2019; Wu et al., 2011) and multiple crop species (Nallamilli et al., 2014; Smith-Hammond et al., 2014) have similarly identified thousands of acetylation events occurring on proteins with diverse functions and subcellular localizations. These two highly abundant PTMs have also been found to intersect on proteins involved in the same cellular processes (Rao et al., 2014; Soufi et al., 2012; Tran et al., 2012; Uhrig et al., 2019) as well as occur on different proteins involved in the same metabolic pathways (Uhrig et al., 2019), suggesting protein phosphorylation and acetylation are functionally intertwined on multiple scales.

To better understand osmotic and salt stress responses in roots, we endeavored to examine the intermediate-term responses (24 h) of *Arabidopsis thaliana* (Arabidopsis) roots subjected to either 300 mM Mannitol or 150 mM NaCl. Then using label-free quantitative (LFQ) proteomics, we quantified the changes in the Arabidopsis root proteome, phosphoproteome, and acetylome. Our findings demonstrate how protein abundance and PTMs change relative to one another and to the transcriptome, in addition to understanding intersections within, and between, each abiotic stress condition to reveal osmotic and/or salt-specific responses.

RESULTS

Quantification and localization of mannitol- and salt-induced protein phosphorylation, acetylation and abundance changes

Twenty-one day old Arabidopsis seedlings grown in liquid MS media were subjected to either osmotic (300 mM mannitol)- or salt (150 mM NaCl)-stress for 24 hours and assessed for quantifiable changes in protein phosphorylation and/or acetylation status as well as protein abundance (Figure 1A). We quantified a total of 3,564 phosphorylated peptides and 281 acetylated peptides across 1,225 and 209 proteins, respectively, with a PTM localization ≥ 0.75 (Supplemental Table 1), while a total of 3,113 proteins were quantified for changes in abundance. Of these, 83 phospho- and 35 acetyl-peptides corresponding to 82 and 33 proteins, respectively, exhibited significant changes under osmotic stress (*pval* ≤ 0.05; FC ≥ 1.5), while 56 phosphorylated and 59 acetylated peptides found on 55 and 56 proteins, respectively, exhibited significant change (*pval* ≤ 0.05; FC ≥ 1.5) under salt stress (Figure 1B-D; Table 1; Supplemental Table 1). A total of 38 and 71 proteins exhibited significant changes in abundance (*pval* ≤ 0.05; FC ≥ 1.5) under osmotic and salt stress (Figure 1B-D; Table 1; Supplemental Table 1).

Next, we compared the Log_2 fold-change (log_2FC) distribution of significantly changing proteins and PTMs between osmotic- and salt-treated roots. This revealed both up- and down-regulation of phosphorylation events and protein abundance, while finding only increases in protein acetylation (Figure 1B-D). Further analysis of proteins exhibiting a significant change in either abundance, phosphorylation or acetylation found a total of 10 (10.2 %), 29 (27.4 %) and 27 (44.3 %) proteins overlapping between stress conditions (Figure 1B-D). Lastly, to understand where intermediate-term changes in the proteome are occurring, we assessed the predicted subcellular localization for all proteins exhibiting a significant change in PTM status or abundance under either osmotic- or salt-stress. Here, we found differences in the subcellular distribution of significantly changing proteins between each treatment (Figure 1E), with mannitol predominantly inducing changes in nuclear, mitochondrial and plasma membrane proteins and salt eliciting greatest change in the plastid and extracellular / ER / Golgi localized proteins (Figure 1E).

Overlap between changing PTMome and proteome is limited

Often, PTMs are quantified independent of assessing changes in proteome abundance. Therefore, reported changes in PTM levels may also be due to fluctuations in protein abundance. To better understand this here, we examined proteins exhibiting PTM changes for concurrent changes in protein abundance. Under osmotic stress 21 (26 %) and 26 (79 %) proteins exhibiting significant changes in either phosphorylation or acetylation were also quantified at the proteome level, however no PTM modified proteins concurrently exhibited a significant change in PTM and protein abundance (Table 1). Similarly, under salt stress, 19 (35 %) and 43 (78 %) phosphorylated and acetylated proteins, respectively, were quantified in our proteome data (Table 1), with only a single acetylated protein exhibiting a concurrent change in protein abundance. Our concurrent assessment of proteome and PTM abundance changes provides increased confidence that observed phosphorylation and acetylation changes are related to PTM-level changes, and not changes in proteome abundance. Moreover, since assessing changes in PTMs requires enrichment of modified peptides, it is likely that the remainder of PTM modified proteins not observed in our protein abundance measurements are simply below detection.

Gene Ontology (GO) analysis of proteome and PTM fluctuations reveals differences between osmotic- and salt-induced stress.

To better understand what cell processes are changing at the proteome-level after 24 h of osmotic or salt stress, we performed a gene ontology (GO) enrichment analysis for biological process GO terms (Supplemental Table 2). In response to salt stress, we found a number of significantly enriched GO terms including: sulfur compound biosynthetic process (GO:0044272), sulfate reduction (GO:0019419), sulfur compound metabolic processes (GO:0006790), seed coat development (GO:0010214), S-glycoside metabolic processes (GO:0016143), glucosinolate metabolic processes (GO:0019757), in addition to metabolic activities related to adenylyl-sulfate reductase activity (GO:0009973) (Table 2).

We then performed a KEGG pathway and protein domain analysis using Thalemine (https://bar.utoronto.ca/thalemine/). Here, we found that proteins involved in primary metabolism, carbon fixation, and amino acid metabolism exhibited significant change in their acetylation status in response to either osmotic or salt stress (Supplemental Table 3). Alternatively, proteins exhibiting a significant change in abundance in response to salt stress alone were enriched in proteins involved in 2-oxocarboxylic acid metabolism or

glucosinolate biosynthesis, supporting our previous GO enrichment analysis (Table 2). Furthermore, we queried our data for enrichment of protein domains and found an enrichment of protein domains amongst proteins significantly changing in abundance under salt stress (Supplemental Table 3). This includes multiple chaperone and chaperonin domains, in addition to glycoside hydrolase domain 35, which supports our GO and KEGG findings of augmented S-glycoside metabolic processes (GO:0016143) in salt stressed roots.

Comparative analysis of proteome and transcriptome changes reveals osmotic and salt-response disconnects.

It is well established that transcriptome and proteome changes are often disconnected in their temporal peak expression patterns (Baerenfaller et al., 2012; Graf et al., 2017; Seaton et al., 2018). Using publicly available microarray transcriptome data from Arabidopsis plants subjected to analogous treatments (Kilian et al., 2007), we performed a comparative analysis to better understand the temporal dynamics of transcripts that correspond to proteins exhibiting phosphorylation, acetylation or abundance changes upon 24 h of osmotic- or salt-stress. Further, we sought to cluster corresponding transcripts based on their expression dynamics and investigate how these dynamics were reflected at the level of protein abundance as well as acetylation or phosphorylation status (Figure 2-3; Supplemental Table 4).

Under both osmotic- and salt-stress conditions, the majority of proteins exhibiting a significant change in abundance, phosphorylation and/or acetylation 24 h post-stress maintained a minimal $\log_2$FC transcriptional change (Cluster 1 - Figure 2-3). We also saw protein clusters emerge under both osmotic- and salt-stress whereby an increasing trend in their transcript abundance from stress onset (0 h) to 24 h post-stress paralleled our observed end-point proteome changes at 24 h (Cluster 2 - Figure 2-3). In the case of osmotic stress, the parallel increase in transcript and protein abundance is also reflected in the protein phosphorylation levels (Cluster 2 - Figure 2).

We then evaluated each cluster for the enrichment of biological process GO terms to uncover how transcriptome and proteome responses may be related. Here, we found enriched GO terms for Cluster 1 of osmotic-stressed roots and Cluster 1 and 2 of salt-stressed roots (Figure 2-3). Under osmotic stress GO terms corresponding to Cluster 1, included multiple metabolic terms (gluconeogenesis; glycolytic process; oxidative phosphorylation) and stress response terms (response to metal ion and temperature) (Figure 2). Comparatively, Cluster 1 and 2 of salt stressed roots were similarly enriched in metabolic processes (gluconeogenesis GO:0006094, glycolysis GO:0006096), in addition to salt-specific terms related to sulfate assimilation (Figure 3).

By clustering the significantly changing proteome and PTMome based on their corresponding transcriptional expression profile from a comparably acquired, publicly available dataset, we find that transcript changes are generally a good indicator of proteome changes 24 h post-osmotic or -salt stress initiation in Arabidopsis roots. Conversely, we find that transcriptional changes are a poor indicator of PTM-level changes. Overall, our data finds that osmotic and salt-stress induced proteomes, when clustered by transcriptional change profile (0 h to 24 h), reveals key differences in how Arabidopsis roots respond to these stresses after 24 h.

Network analysis of proteins exhibiting osmotic- and salt-induced changes in PTM status and/or abundance reveals how the proteomes intersect

Using a combination of STRING-DB association network analyses (https://string-db.org/) and SUBA4 (https://suba.live/) protein subcellular localization information, we assembled subcellular localization-resolved protein association networks to elucidate the degree of interconnectedness between osmotic- and salt-induced PTM and protein abundance changes (Figure 4-5). Proteins with an edge score threshold of 0.5 or below were excluded from visualization. Here, we find that changes in the PTM status and/or protein abundance of metabolic proteins were most common between both osmotic and salt stress conditions (Figure 4-5). This is highlighted by proteins involved in both the transport and assimilation of sulfur as well as carbon metabolism (Figure 4-5). Similarly, changes in RNA processing and protein translation were also common between osmotic and salt treatments, indicating a likely adjustment to transcribed RNAs and a corresponding diversification of translated proteoforms. Conversely, clusters of significantly changing proteins related to sulfur and sucrose metabolism, as well as glucosinolate metabolism, were exclusively found to be salt-induced (Figure 4).

Our association networks further validate earlier GO and KEGG enrichment analyses in addition to visualizing the strength of these relationships using compiled meta-association data between proteins. These networks also provided a means by which to integrate additional data types including: the type and degree of change in acetylation, phosphorylation and/or abundance (outer ring), in addition to the subcellular localization of each protein within the plant cell (inner circle). Together, this data highlights the multi-dimensional relationships that exist between proteins exhibiting significant changes in either abundance or PTM status in response to osmotic and/or salt stress.

Root phenotyping identifies a potential new regulator of root elongation

To validate the findings of our quantitative proteomics workflow, we undertook root phenotypic analysis of an Armadillo repeat protein 2 (ARO2; AT5G66200) insertional mutant (*aro2-1*; SALK_003387). ARO2 exhibited the largest fold-change in abundance (Log_2FC= -2.8) of any protein in our NaCl treatment, rendering it a logical candidate (Supplemental Table 1; Figure 1B; Figure 4). Phenotypic analysis of *aro2-1* root length after growth on 300 mM mannitol and 150 mM NaCl revealed *aro2-1* possessed significantly shorter roots under salt stress by day 11 (n = 100; Student t-test $pval \leq 0.05$) (Figure 6). This is consistent with our hypothesis that by 24 h we are measuring protein-level changes that relate to longer-term adjustments being made by Arabidopsis roots in response to these stresses.

DISCUSSION

Protein acetylation shows unique upward trend under salt and drought stress

Protein acetylation is almost universally upregulated under both osmotic and salt stress (Figure 1B). Many of the acetylated proteins we find here represent core metabolic proteins central to plant survival. For example, under both osmotic and salt treatments, key metabolic enzymes, such as UGP1 and PGK1, were acetylated (Figure 4-5). Protein acetylation has been shown to be a regulatory PTM (Zhao et al., 2010). Catalyzed by acetyltransferases, protein acetylation requires the primary metabolite acetyl-CoA. Acetyl CoA is a central intermediate metabolite between catabolic and anabolic pathways and as such, it is uniquely placed to exert either feedback or feedforward regulation through reversible protein acetylation. Multiple studies have found that

N^{ε} protein acetylation is an abundant PTM across plants (De Boor et al., 2015; Finkemeier et al., 2011; Hartl et al., 2017; Li et al., 2018; Uhrig et al., 2019; Wu et al., 2011). In particular, it was found that the glycolytic and specialized metabolic proteins were extensively acetylated under nitrogen stress in tea leaves (Jiang et al., 2018). N^{α} protein acetylation has also been connected to drought resistance and is suggested to be regulated by ABA stress response (Linster et al., 2015; Linster et al., 2020). However, since both N^{α} and N^{ε} protein acetylation rely on acetyl-CoA as an acetate donor, there are likely some higher-level intersections between these two forms of protein acetylation. Highlighting this possibility are the recent discovery of dual-specificity GNAT Acetyltransferases in Arabidopsis (Bienvenut et al., 2020).

Sulfur metabolism needed for short- and intermediate-term drought response

During drought stress, abscisic acid (ABA) is synthesized in the roots and then transported to the shoots to induce stomatal closure (Agurla et al., 2018). However, ABA biosynthesis in the roots requires sulfur. Plant root sulfate assimilation is primarily driven by adenosine 5′-phosphosulfate reductase (APR), which reduces sulfate to sulfite followed by further reduction to sulfide by ferredoxin dependent sulfite reductase (SiR) (Takahashi et al., 2011). Sulfide is then fixed by O-acetylserine(thiol)lyase into Cysteine (Cys) (Chan et al., 2013) to act as the sulfur donor for the sulfuration of molybdenum cofactor (Moco) sulfurase (Xiong et al., 2001), which is then necessary to initiate abscisic aldehyde oxidase 3 (AAO3) (Mendel, 2002; Schwarz and Mendel, 2006) and the ultimate production of ABA.

Studies have determined that Cys levels attune ABA biosynthesis (Batool et al., 2018; Cao et al., 2014), which in turn, is ultimately limited by sulfur assimilation at the level of APR (Takahashi et al., 2011). APR enzymatic activity is driven by the demand for sulfur, meaning that the uptake and assimilation of sulfur during drought is likely foundational to the short-term drought response. At 24 h of NaCl stress, we observed a number of key sulfur assimilating enzymes decrease in their protein abundance, including: ATP sulfurylase 1 (APS1) (Log_2FC = -1.37), adenosine 5′-phosphosulfate reductase (APR1; Log_2FC = -0.64), APR2 (Log_2FC = -1.69) and APR3 (Log_2FC = -1.75) (Figure 3). This suggests that by 24 h post salt-stress initiation plants have transitioned from utilizing short-term adaptations, to implementing longer term solutions. Transcriptionally, APR is regulated by sulfur availability (Hirai et al., 2003), demand for Cys (Davidian and Kopriva, 2010), and also in response to environmental stressors such as high salt (Koprivova et al., 2008). Specifically, Koprivova and colleagues (2008) reported a 3-fold increase in APR mRNA after 5 h of 150 mM NaCl in Arabidopsis roots. Using the AtGenExpress Arabidopsis stress expression dataset, we calculated a peak expression of APR transcripts at 6 h post 150 mM NaCl stress initiation, which then was found to continually decrease through to 24 h (Kilian et al., 2007; Supplemental Table 4).

Interestingly, an opposing trend in shoot APR expression is observed (Kilian et al., 2007). While APR in roots peaks soon after high salt exposure, APR in shoots remains low until it eventually peaks at 24 h. This points to APR and sulfur driven drought-responses acting as a short-term responder in the roots and an intermediate responder in the shoots. Given this, a sharp increase in root APR levels may facilitate the sulfur assimilation required for ABA production, which then leads to prompt stomatal closure. A later peak in shoot APR may be useful for intermediate drought response mechanisms, such as reducing reactive oxygen species (ROS).

Salt stress is also known to increase the production of oxidative enzymes (e.g. NADPH oxidase), which are necessary for signaling and response during abiotic stress (Mittova et al., 2003), with subsequent reduction in ROS required as the salt stress persists (Hasegawa and Bressan, 2000). To mitigate the damaging effects of ROS, plants can produce glutathione (GSH), an antioxidant derived from Glu, Cys, and Gly. Stress-induced GSH production requires sulfur-containing Cys, with high levels of Cys found to enhance synthesis of GSH in plants (Takahashi et al., 2011). Demand for both, Cys and GSH, reciprocally regulates sulfur assimilation through APR (Davidian and Kopriva, 2010), with depletion of GSH pools under prolonged drought stress conditions driving the production of APR (Chan et al., 2013). Thus, upregulation of APR activity in the shoots may contribute to the production of antioxidants such as GSH. Further time-course experimentation is required to fully elucidate the interplay between salt-induced sulfur metabolism changes at the protein level in roots versus shoots, and is beyond the scope of this study.

Acetylation of ANNAT1 annexin may increase peroxide activity during osmotic stress

Annexins are Ca^{2+} signaling membrane-binding proteins that possess peroxidase activity and are involved in plant drought responses (Mortimer et al., 2008). Overexpression of ANNAT1 in Arabidopsis shoots resulted in enhanced drought tolerance (Konopka-Postupolska et al., 2009) and while under salt stress, ANNAT1 was found to increase in a Ca^{2+} dependent manner (Lee et al., 2004). Furthermore, *annat1* plants are hypersensitive to salt stress and ABA (Konopka-Postupolska et al., 2009; Lee et al., 2004). Under both osmotic and salt treatment we find ANNAT1 to be acetylated ($Log_2FC = 1.801$). Interestingly, Arabidopsis ANNAT1 protein expressed in, and purified from, *Nicotiana benthamiana* had three times more activity than bacterially expressed AtANNAT1, suggesting that PTMs such as protein acetylation or some other binding partner specific to plants, may make the observed peroxidase activity physiologically relevant (Gorecka et al., 2005). Previously, ANNAT1 peroxidase activity was thought to be dependent on phosphorylation events (Kim et al., 2015); however, our evidence suggests that under osmotic stress, acetylation may be a primary regulatory PTM of ANNAT1. Overall, the annexin-peroxidase connection could mean that annexins play a role in limiting the exposure and/or accumulation of ROS during salt or osmotic stress-induced oxidative bursts in plants.

Osmotic and salt stress induce high-levels of UDP-glucose pyrophosphorylase (UGP1) acetylation

We find that UGP1 maintained the second largest increase in acetylation, with salt ($Log_2FC = 4.14$) and osmotic ($Log_2FC = 3.33$) stress both eliciting large changes (Figure 2-3). UGP1 activity has previously been found to be regulated by PTMs. For example, phosphorylation by Per-Arnt-Sim (PAS) kinase downregulates UGP1 activity resulting in a net decrease of glycogen in yeast (Rutter et al., 2002). Analysis of available osmotic- and salt-stress induced transcript data found limited changes in UGP1 transcript levels under mannitol (-0.35) and salt (-0.15) treatments 24 h post stress initiation (Kilian et al., 2007); however, UGP1 transcripts are also known to be a poor indicator of protein-level or enzyme activity changes (Ciereszko et al., 2001).

UGP1 is an ubiquitous enzyme found in plants, animals, and bacteria that produces UDP-glucose (Meng et al., 2009), which is the direct substrate for trehalose synthesis (Schluepmann and Matthew, 2009). Thus, activation of UGP1 may be linked to increased trehalose biosynthesis in osmotic- and salt-stressed roots. In *E. coli,* trehalose stabilizes proteins and prevents protein aggregation during osmotic stress (Moruno Algara et al.,

2019). This is also true for resurrection plants such as *Myrothamnus flabellifolius* where trehalose functions as a protectant to stabilize membranes and proteins, allowing them to survive during dehydration-rehydration cycles (Figueroa and Lunn, 2016; O'Hara et al., 2013). There is evidence that trehalose synthesis in Arabidopsis may serve a similar function during drought stress (Lin et al., 2019). Furthermore, knockdown of UGP1 in *S. cerevisiae* results in a reduction in trehalose as well as a reduction in oxidative stress resistance (Yi and Huh, 2015), suggesting that UGP1 involvement in mitigating osmotic stress is an evolutionary conserved mechanism.

In plants, stachyose and raffinose family oligosaccharides (RFO) are degraded by UGP1 (PWY-6527; https://biocyc.org/), releasing diphosphate. Thus an upregulation of UGP1 protein-levels and/or adjustments to its activity could serve as a homeostatic mechanism for adjusting the nutritional status of a plant under drought stress. Alternatively, if UGP1 acetylation decreases functionality, it may increase RFO content in the cell. RFOs are suggested to have a dual role as osmoprotectants and compatible solutes (Elsayed et al., 2014). Other groups have found higher RFO content in desiccated plant tissues (Obendorf and Gorecki, 2012) and that RFOs stabilize membranes during dehydration (Pluskota et al., 2015). Overall, our data suggests that UGP1 functionality may be regulated by reversible acetylation under both osmotic and salt stress conditions. However, whether UGP1 acetylation increases or decreases UPG1 activity, and how that activity confers osmotic protection, is beyond the scope of this study.

Acetylation of GTP-Proteins may support root tip mitotic division

In Arabidopsis, GTP hydrolysis by Ran and Ran binding protein complexes are important in the regulation of auxin-induced mitotic progression in root tips (Kim and Roux, 2003; Xu et al., 2016). In particular, both AtRAN1 and AtRAN3 are known to both be induced by salt treatment, with *ran1/ran3* double mutants showing higher sensitivity to salt treatment, displaying significantly reduced root growth after being treated for 5 d with 100 mM NaCl. GTPases are also known to directly intersect with ABA response and drought tolerance (Luo et al., 2013).

Our data supports the involvement of RAN-GTPases in osmotic and salt stress responses. In particular, we find SIRANBP and RAN3 to be acetylated under salt (Log_2FC = 2.01 SIRANBP; Log_2FC = 2.46 RAN3) and mannitol (Log_2FC = 2.09 SIRANBP; Log_2FC = 1.55 RAN3) treatment (Figure 2-3). Phylogenetic analysis of RAN-GTPases across Eukaryotes finds a high sequence conservation between higher plants and vertebrates (Coppola et al., 2018), rendering it interesting that Ran GTPases in humans and mice are also regulated by reversible protein acetylation (De Boor et al., 2015). In these cases, increased acetylation of Ran-GTPases prevents the degradation of Ran-GTP, leading to a higher supply of active Ran-GTP that more effectively induces mitosis (De Boor et al., 2015). In particular, the acetylation of RAN-GTPases induces more efficient GTP loading to Ran, which in turn increases Ran-GTPase activity for accurate chromosome-kinetochore attachment (Bao et al., 2018). Therefore, our observation of increased AtRAN-GTPase acetylation may be a mechanism by which the plants are trying to maintain root elongation under drought stress conditions.

Salt-dependent decreases in ARO2 protein abundance conditionally limit root elongation.

ARO2 is a member of the Armadillo repeat-containing proteins (ARCPs), which are conserved across all eukaryotic proteomes, and are typically characterized by domains composed of multiple 42 amino acid Arm repeats (Saito, 2006). ARCPs are involved in diverse cellular processes such as cytoskeletal regulation, signal transduction, and transcription regulation (Mei et al., 2012). Previous research found ARCPs were essential for

proper microtubule assembly needed in areas of active mitosis, such as root tips. CSI1, another member of the ARCPs, stabilizes microtubule assembly required for proper anther formation and root tip elongation (Mei et al., 2012). Microtubular cytoskeleton regulation is not unique to CSI1 but a core characteristic of ARCPs (Sakai et al., 2008; Sapiro et al., 2000). The relationship between microtubular regulation and ARPC was further exemplified by ARO1, an orthologous relative of ARO2. ARO1 plays a key role in the organization of actin cytoskeleton, growth polarization, and pollen tube growth (Gebert et al., 2008), rendering it likely that ARO2, like its ARCP relatives, possess a similar function, but in root tip elongation. Under drought and salinity stress, water acquisition favours deeper root systems (Wasson et al., 2012). Therefore, redistributing root branch density from near-surface to deeper depths by elongating primary roots is essential (Uga et al., 2013). Interestingly, our data indicates that loss of ARO2 is detrimental to root growth under salt-stress conditions, suggesting that ARO2 is a key component of the salt-stress root elongation response in Arabidopsis (Figure 6).

CONCLUSION

Here, we describe proteomic and PTMomic changes occurring in Arabidopsis roots exposed to 300 mM mannitol and 150 mM NaCl for 24 h. By examining intermediate proteome responses, we have uncovered a number of potential regulatory candidates and PTM events that may be key to longer-term survival under osmotic and/or salt stress conditions. This is highlighted by the identification of a new salt-stress dependent root elongation regulator ARO2. Furthermore, protein acetylation has emerged as a potentially interesting PTM in the ability of plants to mount responses to either osmotic- or salt-stress conditions. In undertaking a quantitative analysis of the proteome, phosphoproteome and acetylome, we were able to capture a wide swath of the intermediate term protein responses. Moving forward, understanding the intermediate to long-term responses of either osmotic or salt stress at the protein level through time-course experimentation, is especially important for the development of new climate resilient crops.

MATERIALS & METHODS

Plant Growth and Harvesting

Arabidopsis thaliana Col-0 seeds were imbibed 2 days at 4 ^{o}C in the dark prior to growth in Magenta boxes containing 0.5 x MS media containing 0.5 % (w/v) sucrose. Plants were grown at 22 ^{o}C under a 12 h light : 12 h dark photoperiod for 21 days prior to the application of 0.5 x MS media containing 300 mM mannitol (osmotic) or 150 mM NaCl (salt). Seedlings were grown in either experimental or control media for an additional 24 h. Roots were manually separated from shoots and immediately frozen in liquid N_2. Roots were then ground in a mortar and pestle under liquid N_2 and stored at -80 ^{o}C until further use.

Sample Preparation and PTM Affinity Enrichments

Root tissue (800 mg) was extracted using 1:1.5 w/v extraction buffer (4 % SDS, 50 mM HEPES-KOH pH 8.0, 50 mM DTT). Samples were then processed and digested with trypsin (Promega) as previously described (Uhrig et al., 2019). Subsequent enrichment of phosphorylated or acetylated peptides was performed using titanium dioxide (NP-Ti02; Sachtopore; SNX 030S 005 #9205/1639) and anti-acetylated lysine IgG-coupled agarose (ICP0388; ImmuneChem, https://www.immunechem.com) as previously described (Uhrig et al., 2019), prior to analysis by mass spectrometry.

Liquid Chromatography MS/MS

A total of 1 µg of re-suspended peptide was injected by an Easy-nLC 1000 system (Thermo Scientific) and separated on a Thermo Scientific™ EASY-Spray™ HPLC Column (75 µm x 500 mm; particle size 2.0 µm; E803A). The column was equilibrated with 100 % solvent A (0.1 % formic acid (FA) in water). Peptides were eluted using the following gradient of solvent B (0.1 % FA in ACN): 0-50 min; 0-25 % B, 50-60 min; 25-32 % B, 60-70 min; 32-98 % B at a flow rate of 0.3 µl/min. High accuracy mass spectra were acquired with an Orbitrap Fusion (Thermo Scientific) that was operated in data dependent acquisition mode. All precursor signals were recorded in the Orbitrap using quadrupole transmission in the mass range of 300-1500 m/z. Spectra were recorded with a resolution of 120 000 at 190 m/z, a target value of 4E5 and the maximum cycle time was set to 3 seconds. Data dependent MS/MS were recorded in the linear ion trap using quadrupole isolation with a window of 2 Da and HCD fragmentation with 30 % fragmentation energy. The ion trap was operated in rapid scan mode with a target value of 3E4 and a maximum injection time of 100 ms. Precursor signals were selected for fragmentation with a charge state from +2 to +7 and a signal intensity of at least 1E4. A dynamic exclusion list was used for 30 seconds and maximum parallelizing ion injections was activated.

Mass Spectrometry Data Analysis

Raw data were processed using MaxQuant software (version 1.4.1.2, http://www.maxquant.org/)(Cox and Mann, 2008) and searched against The Arabidopsis Information Resource (TAIR10) protein database concatenated with a decoy database supplemented with contaminants using the Andromeda search engine. Fixed modifications included carbamidomethylation of cysteine residues, while methionine oxidation (all searches), lysine acetylation (acetylated peptide enrichments) and phosphorylated serine / threonine and tyrosine (phosphopeptide enrichments) were set as variable modifications, respectively. One missed cleavage for phosphoproteomic and proteomic measurements and two missed cleavages for lysine-acetylated peptides were permitted. A protein and PSM false discovery rates (FDR) threshold of 1 % was used, while match between runs and re-quantify options were enabled. Further downstream analysis was performed using Perseus version 1.5.5.3 (Tyanova et al., 2016). For all data reverse hits and contaminants were removed, followed by assembly into treatment groups, filtering based on the presence of measured data in at least 2 replicates per group and $\log_2$-transformation with missing values replaced based on the normal distribution function set to default parameters. All PTM analyses utilized a PTM site localization score threshold ≥ 0.75. Significant changes in either protein or PTM peptide levels between each treatment condition and the control samples were assessed by Student's T-test (*pval* ≤ 0.05). Mass spectrometry data acquired for this study can be found at the EMBL proteomic repository Proteomics IDEntifications (PRIDE; https://www.ebi.ac.uk/pride/archive/; PXD019139).

Bioinformatics

To identify the biological functions of proteins changing in abundance, phosphorylation or acetylation, a gene ontology (GO) analysis of biological processes was performed using the ONTOLOGIZER (http://ontologizer.de; (Bauer et al., 2008). A parent–child intersection analysis approach was used (Benjamini–Hochberg *FDR* correction *pval* ≤ 0.05). Clustering of Arabidopsis microarray time-course data was performed using a trajectory-based longitudinal clustering algorithm implemented in the kml-shape package in R (Genolini et al., 2016). For inputs, microarray counts were obtained from (Kilian et al., 2007) and fold changes were calculated

for each time point comparing treated samples versus the controls. The resulting dataset was filtered based on the set of 619 proteins that were found to significantly change in either abundance, phosphorylation or acetylation status at 24 h. The resulting transcript fold-changes over the time-course were used to create four clusters based on the transcript trajectories over the 1, 3, 6, 12 and 24 h time points previously obtained (Kilian et al., 2007). Clustered trajectories and corresponding protein data were plotted using the *ggplot2* and *cowplot* packages in R version 3.3.1 (R Core Team 2016). Further characterization of connections between quantified and significantly changing phospho- and acetyl-proteins was performed through association network analyses using the Cytoscape StringDB plugin StringApp (http://apps.cytoscape.org/apps/stringapp;(Szklarczyk et al., 2017) with a minimum association threshold of 0.5. Cytoscape 3.4 (http://www.cytoscape.org/) visualized networks were then supplemented with subcellular localization data derived from SUBAcon (http://suba.live/; (Hooper et al., 2014)

Arabidopsis *aro2-1* root assay

A. thaliana wild type *Col-0* and insertional mutant (*aro2-1*; SALK_003387) seeds were imbibed for 2 days at 4 ^{o}C. Seeds were then germinated for 4 days under a 12 h light : 12 h dark photoperiod. At the end of the fourth day, seedlings were transferred to either control (0.5 X MS), salt stress (0.5 X MS + 150 mM NaCl), or mannitol stress (0.5 X MS + 300 mM mannitol) plates for vertical growth and phenotypic analysis. Each plate contained 8 WT and *aro2-1* mutant seedlings. The seedlings were grown vertically on a custom, blacked-out 3D printed vertical plate holders to minimize root light exposure. Root length was then measured every day for the following 7 days.

ACKNOWLEDGEMENT

The authors would like to thank the Functional Genomics Center Zurich for helpful discussions and the National Science and Engineering Research Council of Canada (NSERC) for funding this research.

LITERATURE CITED

Agurla, S., Gahir, S., Munemasa, S., Murata, Y., and Raghavendra, A.S. (2018) Mechanism of Stomatal Closure in Plants Exposed to Drought and Cold Stress BT - Survival Strategies in Extreme Cold and Desiccation: Adaptation Mechanisms and Their Applications.

Ashraf, M., and Akram, N.A. (2009) Improving salinity tolerance of plants through conventional breeding and genetic engineering: An analytical comparison. *Biotechnol Adv*. 27: 744–752.

Baerenfaller, K., Massonnet, C., Walsh, S., Baginsky, S., Bühlmann, P., Hennig, L., et al. (2012) Systems-based analysis of Arabidopsis leaf growth reveals adaptation to water deficit. *Mol Syst Biol*. 8.

Bao, X., Liu, H., Liu, X., Ruan, K., Zhang, Y., Zhang, Z., et al. (2018) Mitosis-specific acetylation tunes Ran effector binding for chromosome segregation. *J Mol Cell Biol*. 10: 18–32.

Batool, S., Uslu, V.V., Rajab, H., Ahmad, N., Waadt, R., Geiger, D., et al. (2018) Sulfate is incorporated into cysteine to trigger ABA Production and stomatal closure. *Plant Cell*. 30: 2973–2987.

Bauer, S., Grossmann, S., Vingron, M., and Robinson, P.N. (2008) Ontologizer 2.0 - A multifunctional tool for GO term enrichment analysis and data exploration. *Bioinformatics*. 24: 1650–1651.

Bienvenut, W. V, Brünje, A., Boyer, J., Mühlenbeck, J.S., Bernal, G., Lassowskat, I., et al. (2020) Dual lysine and N-terminal acetyltransferases reveal the complexity underpinning protein acetylation. *Mol Syst Biol*. 16: 1–23.

De Boor, S., Knyphausen, P., Kuhlmann, N., Wroblowski, S., Brenig, J., Scislowski, L., et al. (2015) Small GTP-binding protein Ran is regulated by posttranslational lysine acetylation. *Proc Natl Acad Sci U S A*. 112: E3679–E3688.

Cao, M.J., Wang, Z., Zhao, Q., Mao, J.L., Speiser, A., Wirtz, M., et al. (2014) Sulfate availability affects ABA levels and germination response to ABA and salt stress in Arabidopsis thaliana. *Plant J*. 77: 604–615.

Chan, K.X., Wirtz, M., Phua, S.Y., Estavillo, G.M., and Pogson, B.J. (2013) Balancing metabolites in drought□: the sulfur assimilation conundrum. *Trends Plant Sci*. 18: 18–29.

Choudhary, C., Kumar, C., Gnad, F., Nielsen, M.L., Rehman, M., Walther, T.C., et al. (2009) Lysine acetylation targets protein complexes and co-regulates major cellular functions. *Science (80-)*. 325: 834–840.
Ciereszko, I., Johansson, H., Hurry, V., and Kleczkowski, L.A. (2001) Phosphate status affects the gene expression, protein content and enzymatic activity of UDP-glucose pyrophosphorylase in wild-type and pho mutants of Arabidopsis. *Planta*. 212: 598–605.
Coppola, U., Caccavale, F., Scelzo, M., Holland, N.D., Ristoratore, F., and D'Aniello, S. (2018) Ran GTPase, an eukaryotic gene novelty, is involved in amphioxus mitosis. *PLoS One*. 13: 1–13.
Cox, J., and Mann, M. (2008) MaxQuant enables high peptide identification rates, individualized p.p.b.-range mass accuracies and proteome-wide protein quantification. *Nat Biotechnol*. 26: 1367–1372.
Davidian, J.C., and Kopriva, S. (2010) Regulation of sulfate uptake and assimilation - The same or not the same? *Mol Plant*. 3: 314–325.
Elsayed, A.I., Rafudeen, M.S., and Golldack, D. (2014) Physiological aspects of raffinose family oligosaccharides in plants: Protection against abiotic stress. *Plant Biol*. 16: 1–8.
Figueroa, C.M., and Lunn, J.E. (2016) A tale of two sugars: Trehalose 6-phosphate and sucrose. *Plant Physiol*. 172: 7–27.
Finkemeier, I., Laxa, M., Miguet, L., Howden, A.J.M., and Sweetlove, L.J. (2011) Proteins of diverse function and subcellular location are lysine acetylated in Arabidopsis. *Plant Physiol*. 155: 1779–1790.
Food and Agriculture Organization of the United Nations (FAO) (2017) The Impact of disasters and crises on agriculture and Food Security.
Gebert, M., Dresselhaus, T., and Sprunck, S. (2008) F-actin organization and pollen tube tip growth in Arabidopsis are dependent on the gametophyte-specific armadillo repeat protein ARO1. *Plant Cell*. 20: 2798–2814.
Genolini, C., Ecochard, R., Benghezal, M., Driss, T., Andrieu, S., and Subtil, F. (2016) kmlShape: An efficient method to cluster longitudinal data (Time-Series) according to their shapes. *PLoS One*. 11: 1–24.
Ghosh, D., and Xu, J. (2014) Abiotic stress responses in plant roots: A proteomics perspective. *Front Plant Sci*. 5: 1–13.
Gorecka, K.M., Konopka-Postupolska, D., Hennig, J., Buchet, R., and Pikula, S. (2005) Peroxidase activity of annexin 1 from Arabidopsis thaliana. *Biochem Biophys Res Commun*. 336: 868–875.
Graf, A., Coman, D., Uhrig, R.G., Walsh, S., Flis, A., Stitt, M., et al. (2017) Parallel analysis of *Arabidopsis* circadian clock mutants reveals different scales of transcriptome and proteome regulation. *Open Biol*. 7: 160333.
Hartl, M., Füßl, M., Boersema, P.J., Jost, J., Kramer, K., Bakirbas, A., et al. (2017) Lysine acetylome profiling uncovers novel histone deacetylase substrate proteins in Arabidopsis . *Mol Syst Biol*. 13: 949.
Hasegawa, P.M., and Bressan, R.A. (2000) Plant Cellular and Molecular Responses to High Salinity. *Annu Rev Plant Biol*. 51: 463–499.
Heazlewood, J.I., Durek, P., Hummel, J., Selbig, J., Weckwerth, W., Walther, D., et al. (2008) PhosPhAt□: A database of phosphorylation sites in Arabidopsis thaliana and a plant-specific phosphorylation site predictor. *Nucleic Acids Res*. 36: 1015–1021.
Henriksen, P., Wagner, S.A., Weinert, B.T., Sharma, S., Bačinskaja, G., Rehman, M., et al. (2012) Proteome-wide analysis of lysine acetylation suggests its broad regulatory scope in saccharomyces cerevisiae. *Mol Cell Proteomics*. 11: 1510–1522.
Hirai, M.Y., Fujiwara, T., Awazuhara, M., Kimura, T., Noji, M., and Saito, K. (2003) Global expression profiling of sulfur-starved Arabidopsis by DNA macroarray reveals the role of O-acetyl-L-serine as a general regulator of gene expression in response to sulfur nutrition. *Plant J*. 33: 651–663.
Hooper, C.M., Tanz, S.K., Castleden, I.R., Vacher, M.A., Small, I.D., and Millar, A.H. (2014) SUBAcon: A consensus algorithm for unifying the subcellular localization data of the Arabidopsis proteome. *Bioinformatics*. 30: 3356–3364.
Jiang, J., Gai, Z., Wang, Y., Fan, K., Sun, L., Wang, H., et al. (2018) Comprehensive proteome analyses of lysine acetylation in tea leaves by sensing nitrogen nutrition. *BMC Genomics*. 19: 1–13.
Jiang, Y., Yang, B., Harris, N.S., and Deyholos, M.K. (2007) Comparative proteomic analysis of NaCl stress-responsive proteins in Arabidopsis roots. *J Exp Bot*. 58: 3591–3607.
Kaushal, S.S., Likens, G.E., Pace, M.L., Utz, R.M., Haq, S., Gorman, J., et al. (2018) Freshwater salinization syndrome on a continental scale. *Proc Natl Acad Sci U S A*. 115: E574–E583.
Kilian, J., Whitehead, D., Horak, J., Wanke, D., Weinl, S., Batistic, O., et al. (2007) The AtGenExpress global stress expression data set: Protocols, evaluation and model data analysis of UV-B light, drought and cold stress responses. *Plant J*. 50: 347–363.
Kim, D., Ntui, V.O., Zhang, N., and Xiong, L. (2015) Arabidopsis Yak1 protein (AtYak1) is a dual specificity protein kinase. *FEBS Lett*. 589: 3321–3327.
Kim, S.H., and Roux, S.J. (2003) An Arabidopsis Ran-binding protein, AtRanBP1c, is a co-activator of Ran

GTPase-activating protein and requires the C-terminus for its cytoplasmic localization. *Planta*. 216: 1047–1052.
Koh, J., Chen, G., Yoo, M.J., Zhu, N., Dufresne, D., Erickson, J.E., et al. (2015) Comparative Proteomic Analysis of Brassica napus in Response to Drought Stress. *J Proteome Res*. 14: 3068–3081.
Konopka-Postupolska, D., Clark, G., Goch, G., Debski, J., Floras, K., Cantero, A., et al. (2009) The role of annexin 1 in drought stress in Arabidopsis. *Plant Physiol*. 150: 1394–1410.
Koprivova, A., North, K.A., and Kopriva, S. (2008) Complex signaling network in regulation of adenosine 5′-phosphosulfate reductase by salt stress in arabidopsis roots. *Plant Physiol*. 146: 1408–1420.
Kreps, J.A., Wu, Y., Chang, H.S., Zhu, T., Wang, X., and Harper, J.F. (2002) Transcriptome changes for Arabidopsis in response to salt, osmotic, and cold stress. *Plant Physiol*. 130: 2129–2141.
Lee, S., Lee, E.J., Yang, E.J., Lee, J.E., Park, A.R., Song, W.H., et al. (2004) Proteomic of identification of annexins, calcium-dependent membrane binding proteins that mediate osmotic stress and abscisic acid signal transduction in arabidopsis. *Plant Cell*. 16: 1378–1391.
Li, X., Ye, J., Ma, H., and Lu, P. (2018) Proteomic analysis of lysine acetylation provides strong evidence for involvement of acetylated proteins in plant meiosis and tapetum function. 142–154.
Lin, Q., Yang, J., Wang, Q., Zhu, H., Chen, Z., Dao, Y., et al. (2019) Overexpression of the trehalose-6-phosphate phosphatase family gene AtTPPF improves the drought tolerance of Arabidopsis thaliana. *BMC Plant Biol*. 19: 1–15.
Linster, E., Layer, D., Bienvenut, W. V., Dinh, T. V., Weyer, F. A., Wiebke, L., et al. (2020) The Arabisopsis N-acetyltransferase NAA60 locates to the plasma membrane and is vital for the high salt stress response. *New Phytol*. 2: 554-546.
Linster, E., Stephan, I., Bienvenut, W. V., Maple-Grødem, J., Myklebust, L.M., Huber, M., et al. (2015) Downregulation of N-terminal acetylation triggers ABA-mediated drought responses in Arabidopsis. *Nat Commun*. 6.
Liu, S., Yu, F., Yang, Z., Wang, T., Xiong, H., Chang, C., et al. (2018) Establishment of dimethyl labeling-based quantitative acetylproteomics in Arabidopsis. *Mol Cell Proteomics*. 17: 1010–1027.
Luo, J., Tang, S., Peng, X., Yan, X., Zeng, X., Li, J., et al. (2015) Elucidation of cross-talk and specificity of early response mechanisms to salt and PEG-simulated drought stresses in brassica napus using comparative proteomic analysis. *PLoS One*. 10: 1–24.
Luo, Y., Wang, Z., Ji, H., Fang, H., Wang, S., Tian, L., et al. (2013) An Arabidopsis homolog of importin β1 is required for ABA response and drought tolerance. *Plant J*. 75: 377–389.
Mei, Y., Gao, H.B., Yuan, M., and Xue, H.W. (2012) The Arabidopsis ARCP protein, CSI1, which is required for microtubule stability, is necessary for root and anther development. *Plant Cell*. 24: 1066–1080.
Mendel, R.R. (2002) Molybdoenzymes and molybdenum cofactor in plants. *J Exp Bot*. 53: 1689–1698.
Meng, M., Geisler, M., Johansson, H., Harholt, J., Scheller, H. V., Mellerowicz, E.J., et al. (2009) UDP-glucose pyrophosphorylase is not rate limiting, but is essential in arabidopsis. *Plant Cell Physiol*. 50: 998–1011.
Mergner, J., Frejno, M., List, M., Papacek, M., Chen, X., Chaudhary, A., et al. (2020) Mass-spectrometry-based draft of the Arabidopsis proteome. *Nature*. 579: 409–414.
Mittova, V., Tal, M., Volokita, M., and Guy, M. (2003) Up-regulation of the leaf mitochondrial and peroxisomal antioxidative systems in response to salt-induced oxidative stress in the wild salt-tolerant tomato species Lycopersicon pennellii. *Plant, Cell Environ*. 26: 845–856.
Mortimer, J.C., Laohavisit, A., Macpherson, N., Webb, A., Brownlee, C., Battey, N.H., et al. (2008) Annexins: Multifunctional components of growth and adaptation. *J Exp Bot*. 59: 533–544.
Moruno Algara, M., Kuczyńska-Wiśnik, D., Dębski, J., Stojowska-Swędrzyńska, K., Sominka, H., Bukrejewska, M., et al. (2019) Trehalose protects Escherichia coli against carbon stress manifested by protein acetylation and aggregation. *Mol Microbiol*. 112: 866–880.
Nallamilli, B.R.R., Edelmann, M.J., Zhong, X., Tan, F., Mujahid, H., Zhang, J., et al. (2014) Global analysis of lysine acetylation suggests the involvement of protein acetylation in diverse biological processes in rice (Oryza sativa). *PLoS One*. 9: 1–12.
O'Hara, L.E., Paul, M.J., and Wingler, A. (2013) How do sugars regulate plant growth and development? new insight into the role of trehalose-6-phosphate. *Mol Plant*. 6: 261–274.
Obendorf, R.L., and Gorecki, R.J. (2012) Soluble carbohydrates in legume seeds. *Seed Sci Res*. 22: 219–242.
Paez-Garcia, A., Motes, C.M., Scheible, W.R., Chen, R., Blancaflor, E.B., and Monteros, M.J. (2015) Root traits and phenotyping strategies for plant improvement. *Plants*. 4: 334–355.
Petricka, J.J., Schauer, M.A., Megraw, M., Breakfield, N.W., Thompson, J.W., Georgiev, S., et al. (2012) The protein expression landscape of the Arabidopsis root. *Proc Natl Acad Sci U S A*. 109: 6811–6818.
Pluskota, W.E., Szablińska, J., Obendorf, R.L., Górecki, R.J., and Lahuta, L.B. (2015) Osmotic stress induces genes, enzymes and accumulation of galactinol, raffinose and stachyose in seedlings of pea (Pisum sativum L.). *Acta Physiol Plant*. 37.

Rao, R.S.P., Thelen, J.J., and Miernyk, J.A. (2014) Is Lys-Ne{open}-acetylation the next big thing in post-translational modifications? *Trends Plant Sci*. 19: 550–553.
Reiland, S., Messerli, G., Baerenfaller, K., Gerrits, B., Endler, A., Grossmann, J., et al. (2009) Large-scale arabidopsis phosphoproteome profiling reveals novel chloroplast kinase substrates and phosphorylation networks1[w]. *Plant Physiol*. 150: 889–903.
Rest, J.S., Wilkins, O., Yuan, W., Purugganan, M.D., and Gurevitch, J. (2016) Meta-analysis and meta-regression of transcriptomic responses to water stress in Arabidopsis. *Plant J*. 85: 548–560.
Rutter, J., Probst, B.L., and McKnight, S.L. (2002) Coordinate regulation of sugar flux and translation by PAS kinase. *Cell*. 111: 17–28.
Saito, K. (2006) Sulfur Assimilatory Metabolism. The Long and Smelling Road. 136: 2443–2450.
Sakai, T., Honing, H. Van Der, Nishioka, M., Uehara, Y., Takahashi, M., Fujisawa, N., et al. (2008) Armadillo repeat-containing kinesins and a NIMA-related kinase are required for epidermal-cell morphogenesis in Arabidopsis. *Plant J*. 53: 157–171.
Sapiro, R., Tarantino, L.M., Velazquez, F., Kiriakidou, M., Hecht, N.B., Bucan, M., et al. (2000) Sperm antigen 6 is the murine homologue of the Chlamydomonas reinhardtii central apparatus protein encoded by the PF16 locus. *Biol Reprod*. 62: 511–518.
Schluepmann, H., and Matthew, P. (2009) Trehalose Metabolites in Arabidopsis — elusive , active and central Published By□: The American Society of Plant Biologists Trehalose Metabolites in Arabidopsis — elusive , active and central. 7.
Schwalm, C.R., Anderegg, W.R.L., Michalak, A.M., Fisher, J.B., Biondi, F., Koch, G., et al. (2017) Global patterns of drought recovery. *Nature*. 548: 202–205.
Schwarz, G., and Mendel, R.R. (2006) Molybdenum Cofactor Biosynthesis and Molybdenum Enzymes. *Annu Rev Plant Biol*. 57: 623–647.
Seaton, D.D., Graf, A., Baerenfaller, K., Stitt, M., Millar, A.J., and Gruissem, W. (2018) Photoperiodic control of the Arabidopsis proteome reveals a translational coincidence mechanism . *Mol Syst Biol*. 14: 1–19.
Sharma, K., D'Souza, R.C.J., Tyanova, S., Schaab, C., Wiśniewski, J.R., Cox, J., et al. (2014) Ultradeep Human Phosphoproteome Reveals a Distinct Regulatory Nature of Tyr and Ser/Thr-Based Signaling. *Cell Rep*. 8: 1583–1594.
Shelden, M.C., Dias, D.A., Jayasinghe, N.S., Bacic, A., and Roessner, U. (2016) Root spatial metabolite profiling of two genotypes of barley (Hordeum vulgare L.) reveals differences in response to short-term salt stress. *J Exp Bot*. 67: 3731–3745.
Smith-Hammond, C.L., Swatek, K.N., Johnston, M.L., Thelen, J.J., and Miernyk, J.A. (2014) Initial description of the developing soybean seed protein Lys-Nε-acetylome. *J Proteomics*. 96: 56–66.
Soufi, B., Soares, N.C., Ravikumar, V., and Macek, B. (2012) Proteomics reveals evidence of cross-talk between protein modifications in bacteria: Focus on acetylation and phosphorylation. *Curr Opin Microbiol*. 15: 357–363.
Szklarczyk, D., Morris, J.H., Cook, H., Kuhn, M., Wyder, S., Simonovic, M., et al. (2017) The STRING database in 2017: Quality-controlled protein-protein association networks, made broadly accessible. *Nucleic Acids Res*. 45: D362–D368.
Takahashi, H., Kopriva, S., Giordano, M., Saito, K., and Hell, R. (2011) Sulfur Assimilation in Photosynthetic Organisms: Molecular Functions and Regulations of Transporters and Assimilatory Enzymes. *Annu Rev Plant Biol*. 62: 157–184.
Tran, H.T., Nimick, M., Uhrig, R.G., Templeton, G., Morrice, N., Gourlay, R., et al. (2012) Arabidopsis thaliana histone deacetylase 14 (HDA14) is an α-tubulin deacetylase that associates with PP2A and enriches in the microtubule fraction with the putative histone acetyltransferase ELP3. *Plant J*. 71: 263–272.
Tyanova, S., Temu, T., Sinitcyn, P., Carlson, A., Hein, M.Y., Geiger, T., et al. (2016) The Perseus computational platform for comprehensive analysis of (prote)omics data. *Nat Methods*. 13: 731–740.
Uga, Y., Sugimoto, K., Ogawa, S., Rane, J., Ishitani, M., Hara, N., et al. (2013) Control of root system architecture by DEEPER ROOTING 1 increases rice yield under drought conditions. *Nat Genet*. 45: 1097–1102.
Uhrig, R.G., Schläpfer, P., Roschitzki, B., Hirsch-Hoffmann, M., and Gruissem, W. (2019) Diurnal changes in concerted plant protein phosphorylation and acetylation in Arabidopsis organs and seedlings. *Plant J*. 99: 176–194.
Wasson, A.P., Richards, R.A., Chatrath, R., Misra, S.C., Prasad, S.V.S., Rebetzke, G.J., et al. (2012) Traits and selection strategies to improve root systems and water uptake in water-limited wheat crops. *J Exp Bot*. 63: 3485–3498.
Weinert, B.T., Wagner, S.A., Horn, H., Henriksen, P., Liu, W.R., Olsen, J. V., et al. (2011) Proteome-wide mapping of the Drosophila acetylome demonstrates a high degree of conservation of lysine acetylation. *Sci Signal*. 4: 1–12.
Willems, P., Horne, A., Van Parys, T., Goormachtig, S., De Smet, I., Botzki, A., et al. (2019) The Plant PTM

Viewer, a central resource for exploring plant protein modifications. *Plant J*. 99: 752–762.
Wu, X., Gong, F., Cao, D., Hu, X., and Wang, W. (2016) Advances in crop proteomics: PTMs of proteins under abiotic stress. *Proteomics*. 16: 847–865.
Wu, X., Oh, M.H., Schwarz, E.M., Larue, C.T., Sivaguru, M., Imai, B.S., et al. (2011) Lysine acetylation is a widespread protein modification for diverse proteins in Arabidopsis. *Plant Physiol*. 155: 1769–1778.
Xiong, L., Ishitani, M., Lee, H., and Zhu, J.K. (2001) The Arabidopsis LOS5/ABA3 locus encodes a molybdenum cofactor sulfurase and modulates cold stress- and osmotic stress-responsive gene expression. *Plant Cell*. 13: 2063–2083.
Xu, P., Cai, X.T., Wang, Y., Xing, L., Chen, Q., and Xiang, C. Bin (2014) HDG11 upregulates cell-wall-loosening protein genes to promote root elongation in Arabidopsis. *J Exp Bot*. 65: 4285–4295.
Xu, P., Zang, A., Chen, H., and Cai, W. (2016) The small G protein AtRAN1 regulates vegetative growth and stress tolerance in arabidopsis thaliana. *PLoS One*. 11: 1–15.
Yi, D.G., and Huh, W.K. (2015) UDP-glucose pyrophosphorylase Ugp1 is involved in oxidative stress response and long-term survival during stationary phase in Saccharomyces cerevisiae. *Biochem Biophys Res Commun*. 467: 657–663.
Yin, H., Li, M., Li, D., Khan, S.A., Hepworth, S.R., and Wang, S.M. (2019) Transcriptome analysis reveals regulatory framework for salt and osmotic tolerance in a succulent xerophyte. *BMC Plant Biol*. 19: 1–15.
Zhang, H., Han, B., Wang, T., Chen, S., Li, H., Zhang, Y., et al. (2012) Mechanisms of plant salt response: Insights from proteomics. *J Proteome Res*. 11: 49–67.
Zhao, S., Xu, W., Jiang, W., Yu, W., Lin, Y., Zhang, T., et al. (2010) Regulation of Cellular Metabolism by Protein Lysine Acetylation. *Science (80-)*. 1000–1004.
Zhu, J.K. (2016) Abiotic Stress Signaling and Responses in Plants. *Cell*. 167: 313–324.

TABLES

Table 1: Summary results of proteomic and PTMomics analyses of Arabidopsis roots after 24 hours of salt and osmotic stress.

Stress	Proteome Assessed	*Quantified		**Significantly Changing under Stress		% Sig PTM Quantified not changing in Proteome	% Sig PTM Quantified changing in Proteome
		Proteins	Peptides	Proteins	Peptides	Proteins	Proteins
300mM Mannitol (Osmotic)	Acetylproteome (Ac)	209	281	33	35	26 (79%)	0 (0%)
	Phosphoproteome (P)	1225	3564	81	86	21 (26%)	0 (0%)
	Proteome (TP)	3113	n/a	38	*n/a*	*n/a*	*n/a*
150mM NaCl (Salinity)	Acetylproteome (Ac)	209	281	55	59	43 (78%)	1 (1.8%)
	Phosphoproteome (P)	1225	3564	54	56	19 (35%)	0 (0%)
	Proteome (TP)	3113	*n/a*	71	*n/a*	*n/a*	*n/a*

*Quantified PTM (Ac & P) = Localization ≥ 0.75
*Quantified Proteome (TP) = min 2 peptides per protein
**Significantly changing under stress (Ac, P & TP) = *p-val* ≤ 0.05 and ≥ 1.5 fold-change in PTM abundance

Table 2: Enriched GO terms for significant protein abundance changes upon 24 hours of 150 mM salt (NaCl) treatment

GO Term	GO ID	pvalue	BH pvalue
sulfur compound biosynthetic process	GO:0044272	2.56E-05	0.009996086447
sulfate reduction	GO:0019419	3.33E-05	0.009996086447
sulfur compound metabolic process	GO:0006790	5.79E-05	0.01302706954
adenylyl-sulfate reductase activity	GO:0009973	7.55E-05	0.0135910601
seed coat development	GO:0010214	1.26E-04	0.01736891571
S-glycoside metabolic process	GO:0016143	1.35E-04	0.01736891571
glycosinolate metabolic process	GO:0019757	1.80E-04	0.02021935016
sulfate assimilation	GO:0000103	4.64E-04	0.04180239927
Pathway Description	AGI	Pathway	BH pvalue
2-Oxocarboxylic acid metabolism	AT1G23310, AT1G65930, AT2G20610, AT2G31810, AT2G42790, AT3G19710, AT3G58610, AT4G13770, AT5G11520, AT5G14200, AT5G23010, AT5G23020	1210	0.001175924641
Glucosinolate biosynthesis	AT1G18590, AT2G20610, AT3G19710, AT4G13770, AT5G23010, AT5G23020	966	0.002252925854

Protein Domain Name	AGI	Domain	BH pvalue
Chaperonin TCP-1, conserved site	AT1G24510, AT3G02530, AT3G11830,AT3G20050, AT5G20890, AT5G26360	IPR002194	0.00000773058189
GroEL-like equatorial domain	AT1G24510, AT3G02530, AT3G11830, AT3G20050, AT5G20890, AT5G26360, AT5G56500	IPR027413	0.00001576681032
Chaperonin Cpn60/TCP-1 family	AT1G24510, AT3G02530, AT3G11830, AT3G20050, AT5G20890, AT5G26360, AT5G56500	IPR002423	0.00005815154064
GroEL-like apical domain	AT1G24510, AT3G02530, AT3G11830, AT3G20050, AT5G20890, AT5G26360, AT5G56500	IPR027409	0.00005815154064
Glycoside hydrolase superfamily	AT1G47600, AT1G78060, AT2G32810, AT3G09260, AT3G13750, AT3G18080, AT3G60130, AT4G19810, AT5G08380, AT5G11720, AT5G26000, AT5G49360, AT5G56870, AT5G63800, AT5G63810	IPR017853	0.001488229715
Thioredoxin-independent 5'-adenylylsulphate reductase	AT1G62180, AT4G04610, AT4G21990	IPR004508	0.003244018163
Phosphoadenosine phosphosulphate reductase	AT1G62180, AT4G04610, AT4G21990	IPR002500	0.009327460679
Alkaline-phosphatase-like, core domain	AT1G09780, AT3G03530, AT4G29690, AT4G29700	IPR017850	0.036840083

FIGURES

Figure 1:

Proteome and PTMome changes under osmotic or salt stress. (A) Experimental workflow (B-D) Venn diagram and Log_2 fold-change (FC) scatterplots for significantly changing (B) acetylome, (C) phosphoproteome and (D) proteome. (E) Subcellular localization distribution of significantly changing proteins (*pval* ≤ 0.05; FC ≥ 1.5).

Figure 2:

Comparison of transcript-level changes with corresponding protein abundance, phosphorylation, and acetylation changes upon 24 hours of osmotic stress. Transcript-level changes corresponding to significantly changing proteins were calculated from previously described microarray experiments (KIllan et al., 2007) and clustered by longitudinal shape. Significantly enriched GO terms (Biological process) for each cluster were obtained from geneontology.org.

Figure 3:

Comparison of transcript-level changes with corresponding protein abundance, phosphorylation, and acetylation changes upon 24 hours of salt stress. Transcript-level changes corresponding significantly changing proteins were calculated from previously described microarray experiments (Killan et al., 2007) and clustered by longitudinal shape. Significantly enriched GO terms (Biological process) for each cluster were obtained from geneontology.org.

Figure 4:

Association network of Arabidopsis root under 24 h 150 mM salt (NaCl). STRING database association network shown for proteins significantly changing in their total protein, phosphorylation, or acetylation status. The maximal log_2FC change ranges from -2.5 (Max log_2FC EN) to +2.5 (Max log_2FC ED). Edge thickness equates to confidence in association. Inner circle represents subcellular localization (SUBA 4; https://suba.live/): cytosol (red), mitochondria (purple), nucleus (blue), peroxisome (green), plasma membrane (beige), plastid (amber), vacuole (lavender), endoplasmic reticulum/extracellular/Golgi (grey). Outer ring represents protein status: total protein change (1st division), phosphorylation (2nd division), Acetylation (3rd division). Grey clusters depict proteins belonging to a common cellular process. Proteins with an edge score threshold of 0.5 or below were excluded from visualization.

Figure 5:

Association network of Arabidopsis root under 24 h 300 mM mannitol. STRING database association network shown for proteins significantly changing in their total protein, phosphorylation, or acetylation status. The maximal log_2FC change ranges from -2.5 (Max log_2FC EN) to +2.5 (Max log_2FC ED). Edge thickness equates to confidence in association. Inner circle represents subcellular localization (SUBA 4; https://suba.live/): cytosol (red), mitochondria (purple), nucleus (blue), peroxisome (green), plasma membrane (beige), plastid (amber), vacuole (lavender), endoplasmic reticulum/extracellular/Golgi (grey). Outer ring represents protein status: total protein change (1st division), phosphorylation (2nd division), Acetylation (3rd division). Grey clusters depict proteins belonging to a common cellular process. Proteins with an edge score threshold of 0.5 or below were excluded from visualization.

Figure 6:

Root phenotypes of *aro2-1* and wild-type Arabidopsis under osmotic and salt stress. Root length (cm) of WT and *aro2-1* was measured every day for 11 days. (*:Unpaired t-test *pval* ≤ 0.05 with Holms-Bonferroni correction).

SUPPLEMENTAL INFORMATION

Supplemental Table 1: Results of proteome and PTMome analysis, including proteins with significantly changing protein abundance, phosphorylation and acetylation.

Supplemental Table 2: Gene Ontology enrichment for proteins with significantly changing abundance upon osmotic and salt stress.

Supplemental Table 3: KEGG pathway and protein domain analysis

Supplemental Table 4: Transcript data clustering analysis

770

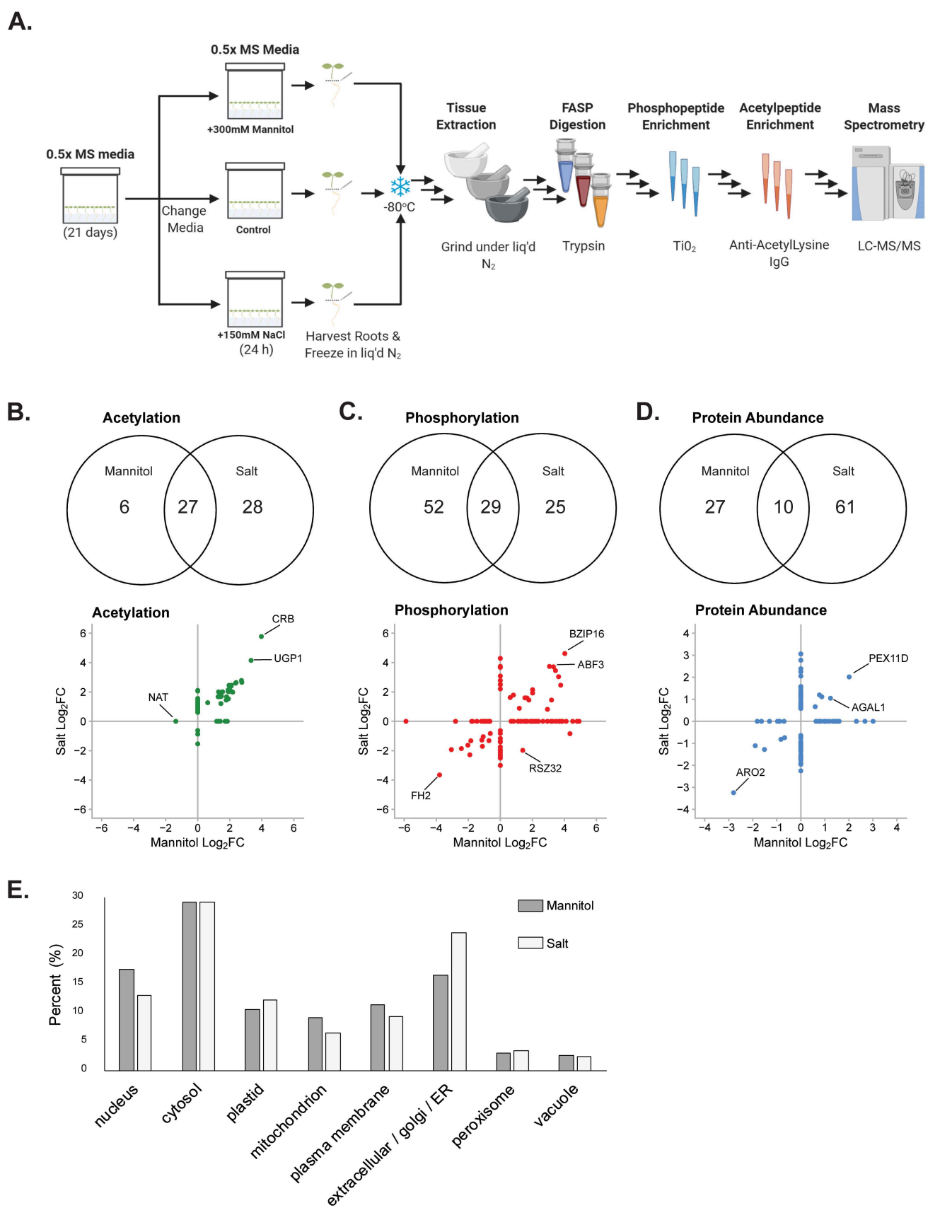
A.
0.5x MS Media
+300mM Mannitol
0.5x MS media
(21 days)
Change Media
Control
+150mM NaCl
(24 h)
Harvest Roots & Freeze in liq'd N2
-80°C
Tissue Extraction
Grind under liq'd N2
FASP Digestion
Trypsin
Phosphopeptide Enrichment
TiO2
Acetylpeptide Enrichment
Anti-AcetylLysine IgG
Mass Spectrometry
LC-MS/MS
B.
Acetylation
Mannitol
Salt
6
27
28
Acetylation
CRB
UGP1
NAT
Salt Log2FC
Mannitol Log2FC
C.
Phosphorylation
Mannitol
Salt
52
29
25
Phosphorylation
BZIP16
ABF3
RSZ32
FH2
Salt Log2FC
Mannitol Log2FC
D.
Protein Abundance
Mannitol
Salt
27
10
61
Protein Abundance
PEX11D
AGAL1
ARO2
Salt Log2FC
Mannitol Log2FC
E.
Percent (%)
Mannitol
Salt
nucleus
cytosol
plastid
mitochondrion
plasma membrane
extracellular / golgi / ER
peroxisome
vacuole

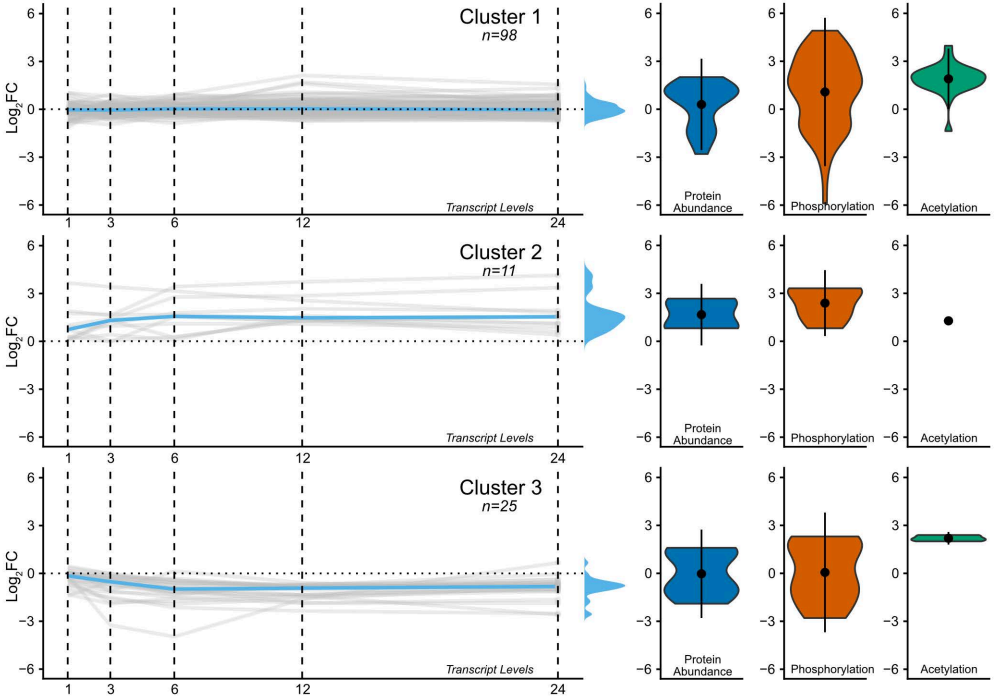

Gene Ontology (Biological Process)	FDR
Response to temperature stimulus	4.02E-02
Response to metal ion	2.53E-02
Positive regulation of oxidative phosphorylation	2.46E-02
Glycolytic Process	1.89E-02
Cellular response to starvation	1.45E-02
Gluconeogenesis	1.02E-02

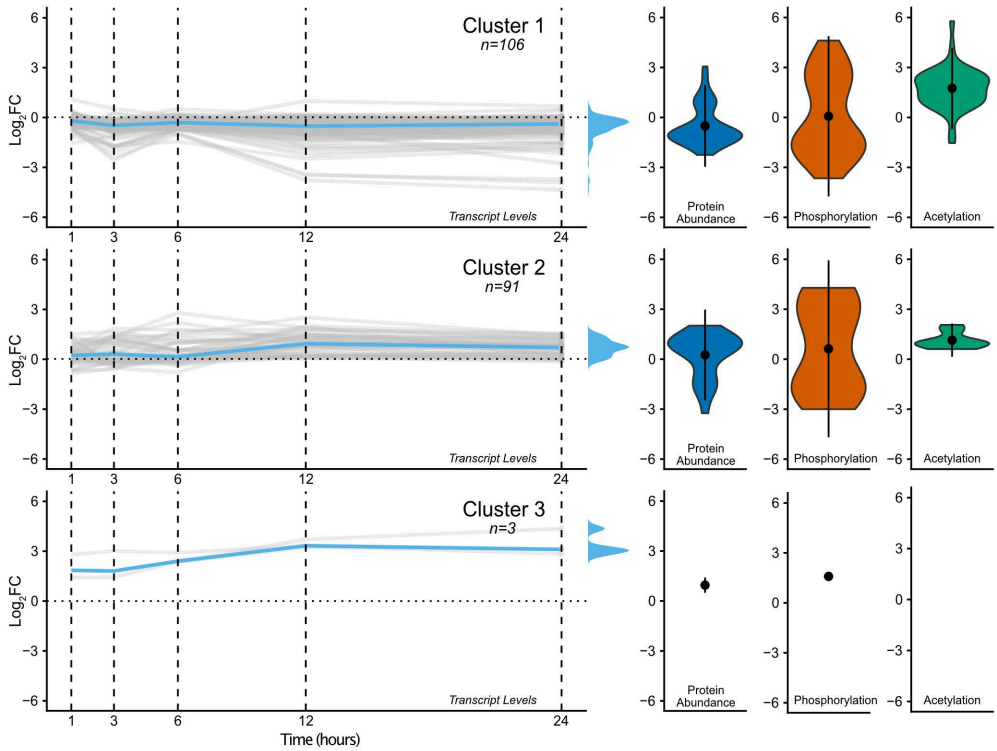

Gene Ontology (Biological Process)	FDR
Response to cadmium ion	5.58E-02
Glucosinolate biosynthetic process	4.75E-02
Response to oxygen containing compound	4.36E-02
Pentose phosphate shunt	3.76E-02
Actin-filament severing	3.61E-02
Ribonucleoprotein complex biogenesis	3.37E-02
Cellular component organisation	2.07E-02
Glycolytic process	2.00E-02
Gluconeogenesis	1.89E-02

Gene Ontology (Biological Process)	FDR
Sulfate assimilation	5.48E-04
Sulfate reduction	4.28E-04

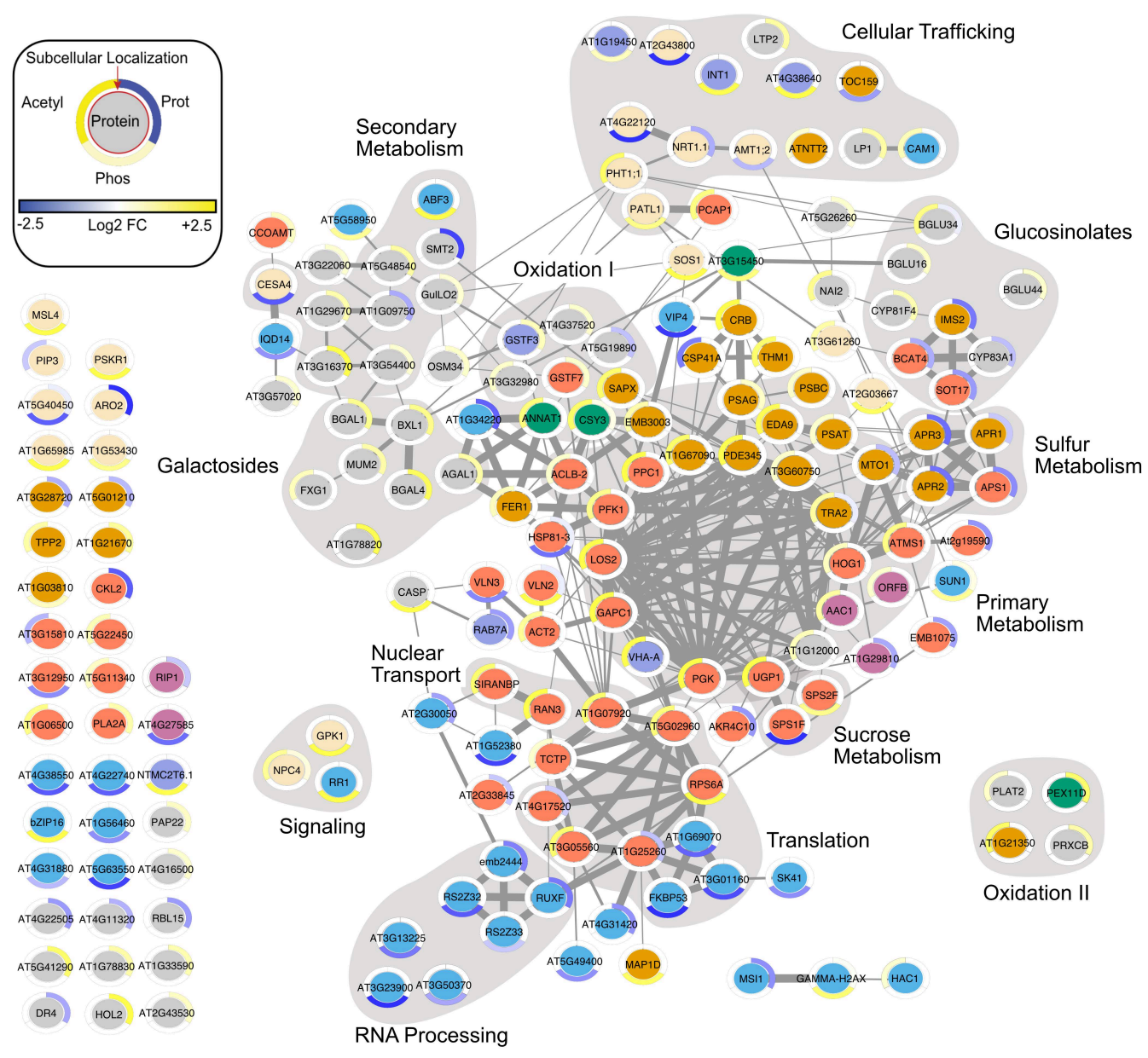

Subcellular Localization
Acetyl
Prot
Protein
Phos
-2.5
Log2 FC
+2.5
Cellular Trafficking
Secondary Metabolism
Oxidation I
Glucosinolates
Sulfur Metabolism
Galactosides
Primary Metabolism
Nuclear Transport
Sucrose Metabolism
Signaling
Translation
Oxidation II
RNA Processing
AT1G19450
AT2G43800
LTP2
INT1
AT4G38640
TOC159
AT4G22120
NRT1.1
AMT1;2
ATNTT2
LP1
CAM1
PHT1;1
PATL1
PCAP1
AT5G26260
BGLU34
BGLU16
BGLU44
NAI2
CYP81F4
IMS2
BCAT4
CYP83A1
SOT17
AT2G03667
APR3
APR1
APR2
APS1
MTO1
ATMS1
At2g19590
HOG1
ORFB
SUN1
AAC1
EMB1075
AT1G12000
AT1G29810
SPS2F
SPS1F
AKR4C10
UGP1
PGK
AT5G02960
AT1G07920
RPS6A
AT1G69070
AT1G25260
AT3G01160
SK41
FKBP53
AT4G31420
MAP1D
AT5G49400
AT3G13225
AT3G23900
AT3G50370
RS2Z32
RS2Z33
RUXF
emb2444
AT3G05560
AT2G33845
AT4G17520
TCTP
AT1G52380
AT2G30050
RAN3
SIRANBP
VHA-A
GAPC1
ACT2
RAB7A
VLN3
VLN2
CASP
LOS2
HSP81-3
FER1
PFK1
PPC1
ACLB-2
AGAL1
BGAL4
FXG1
MUM2
AT1G78820
BGAL1
BXL1
AT1G34220
ANNAT1
CSY3
EMB3003
AT1G67090
PDE345
AT3G60750
TRA2
EDA9
PSAT
PSAG
PSBC
THM1
CSP41A
VIP4
CRB
SAPX
GSTF7
AT3G32980
OSM34
GSTF3
AT4G37520
AT5G19890
AT3G61260
AT3G16370
AT3G54400
IQD14
AT3G57020
CESA4
AT1G29670
AT1G09750
GulLO2
SMT2
AT5G58950
ABF3
CCOAMT
AT3G22060
AT5G48540
AT1G19450
AT2G43800
MSL4
PIP3
PSKR1
AT5G40450
ARO2
AT1G65985
AT1G53430
AT3G28720
AT5G01210
TPP2
AT1G21670
AT1G03810
CKL2
AT3G15810
AT5G22450
AT3G12950
AT5G11340
RIP1
AT1G06500
PLA2A
AT4G27585
AT4G38550
AT4G22740
NTMC2T6.1
bZIP16
AT1G56460
PAP22
AT4G31880
AT5G63550
AT4G16500
AT4G22505
AT4G11320
RBL15
AT5G41290
AT1G78830
AT1G33590
DR4
HOL2
AT2G43530
GPK1
NPC4
RR1
PLAT2
PEX11D
AT1G21350
PRXCB
MSI1
GAMMA-H2AX
HAC1

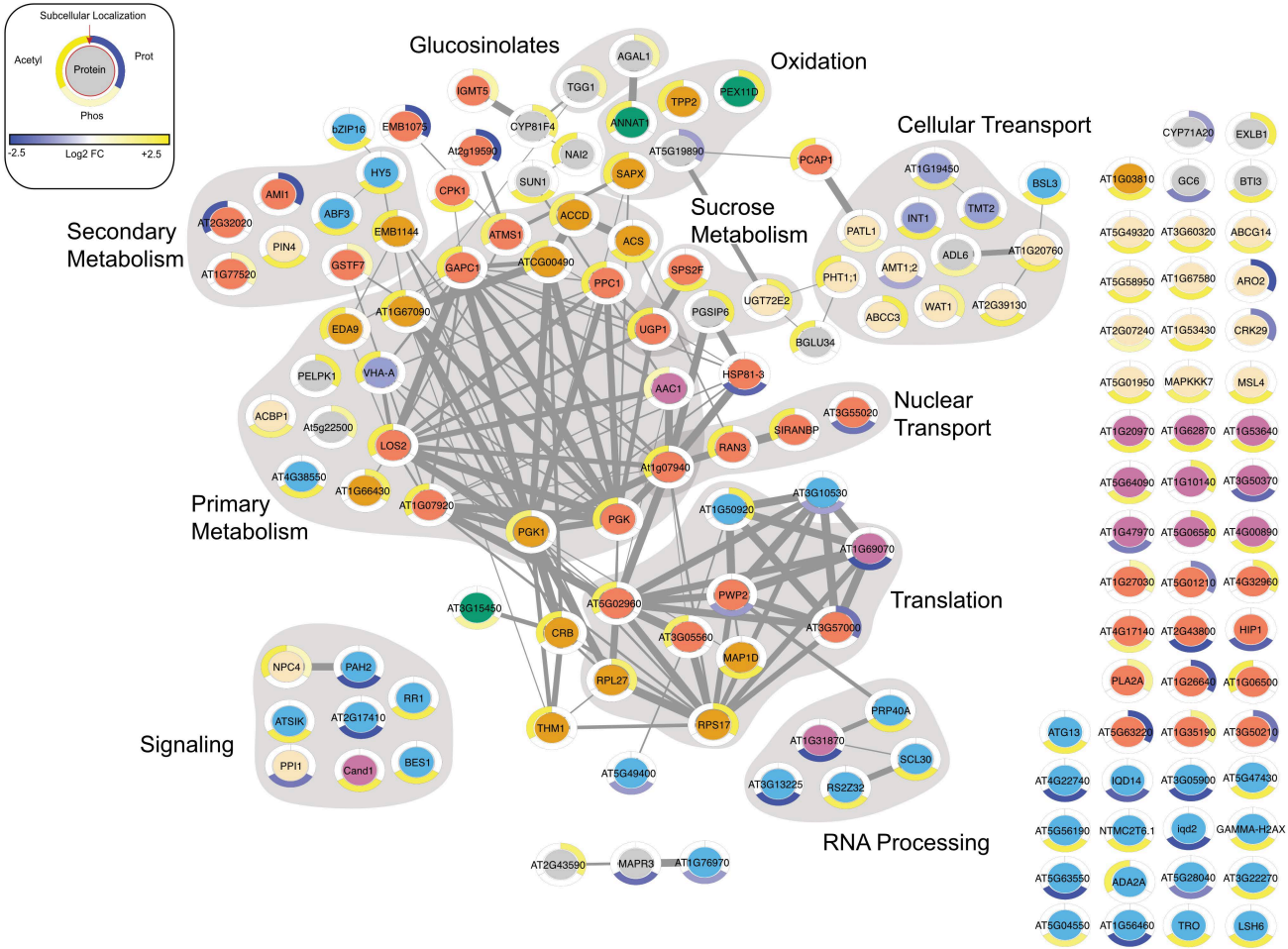

Subcellular Localization
Acetyl
Protein
Prot
Phos
-2.5
Log2 FC
+2.5
Glucosinolates
Oxidation
Cellular Treansport
Secondary Metabolism
Sucrose Metabolism
Nuclear Transport
Primary Metabolism
Translation
Signaling
RNA Processing
AGAL1
IGMT5
TGG1
TPP2
PEX11D
bZIP16
EMB1075
CYP81F4
ANNAT1
At2g19590
NAI2
AT5G19890
PCAP1
HY5
SUN1
SAPX
AMI1
CPK1
ACCD
ABF3
AT2G32020
EMB1144
ATMS1
ACS
PIN4
GSTF7
GAPC1
ATCG00490
SPS2F
AT1G77520
PPC1
AT1G67090
PGSIP6
UGT72E2
EDA9
UGP1
BGLU34
PELPK1
VHA-A
HSP81-3
AAC1
ACBP1
At5g22500
AT3G55020
SIRANBP
LOS2
RAN3
At1g07940
AT4G38550
AT1G66430
AT1G07920
AT3G10530
AT1G50920
PGK
PGK1
AT1G69070
PWP2
AT3G15450
AT5G02960
CRB
AT3G05560
AT3G57000
MAP1D
NPC4
PAH2
RR1
RPL27
ATSIK
AT2G17410
THM1
RPS17
PRP40A
AT1G31870
SCL30
PPI1
Cand1
BES1
AT5G49400
AT3G13225
RS2Z32
AT2G43590
MAPR3
AT1G76970
AT1G19450
BSL3
TMT2
INT1
PATL1
ADL6
AT1G20760
AMT1;2
PHT1;1
WAT1
AT2G39130
ABCC3
CYP71A20
EXLB1
AT1G03810
GC6
BTI3
AT5G49320
AT3G60320
ABCG14
AT5G58950
AT1G67580
ARO2
AT2G07240
AT1G53430
CRK29
AT5G01950
MAPKKK7
MSL4
AT1G20970
AT1G62870
AT1G53640
AT5G64090
AT1G10140
AT3G50370
AT1G47970
AT5G06580
AT4G00890
AT1G27030
AT5G01210
AT4G32960
AT4G17140
AT2G43800
HIP1
PLA2A
AT1G26640
AT1G06500
ATG13
AT5G63220
AT1G35190
AT3G50210
AT4G22740
IQD14
AT3G05900
AT5G47430
AT5G56190
NTMC2T6.1
iqd2
GAMMA-H2AX
AT5G63550
ADA2A
AT5G28040
AT3G22270
AT5G04550
AT1G56460
TRO
LSH6

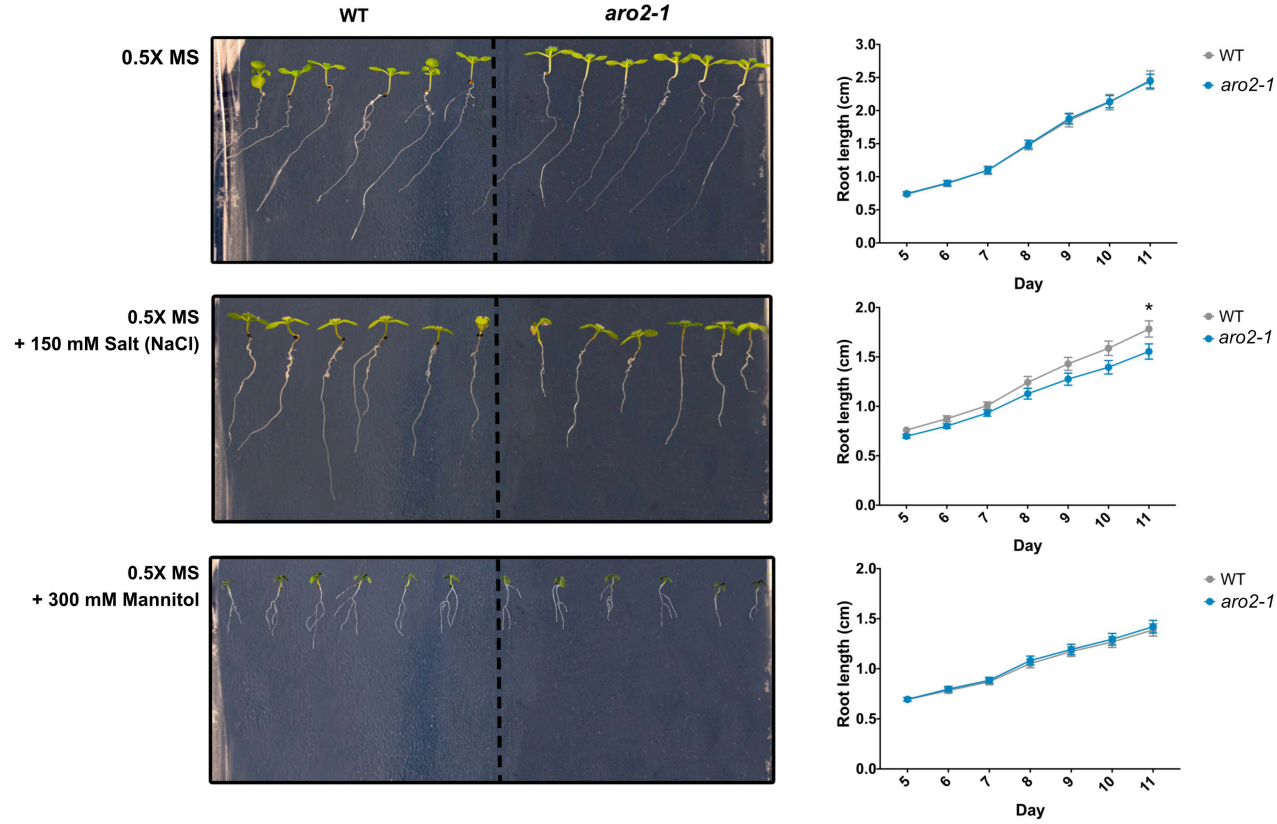
WT
aro2-1
0.5X MS
0.5X MS
+ 150 mM Salt (NaCl)
0.5X MS
+ 300 mM Mannitol
Root length (cm)
Day
WT
aro2-1
*